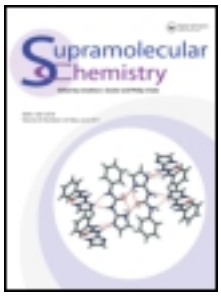

Supramolecular Chemistry
Publication details, including instructions for authors and subscription information:
http://www.tandfonline.com/loi/gsch20

# Effect of bridging anions on the structure and stability of phenoxide bridged zinc dipicolylamine coordination complexes

Edward J. O'Neil [a], Hua Jiang [a b] & Bradley D. Smith [a]

[a] Department of Chemistry and Biochemistry, University of Notre Dame, 2365 Nieuwland Science Hall, Notre Dame, IN, 46556, USA

[b] Beijing National Laboratory for Molecular Sciences, CAS Key Laboratory of Photochemistry, Institute of Chemistry, Chinese Academy of Sciences, Beijing, 100190, P.R. China

Version of record first published: 12 Mar 2013.

To cite this article: Edward J. O'Neil , Hua Jiang & Bradley D. Smith (2013): Effect of bridging anions on the structure and stability of phenoxide bridged zinc dipicolylamine coordination complexes, Supramolecular Chemistry, DOI:10.1080/10610278.2013.776170

To link to this article: http://dx.doi.org/10.1080/10610278.2013.776170

*Supramolecular Chemistry*, 2013
http://dx.doi.org/10.1080/10610278.2013.776170



# Effect of bridging anions on the structure and stability of phenoxide bridged zinc dipicolylamine coordination complexes

Edward J. O'Neil[a], Hua Jiang[a,b] and Bradley D. Smith[a]*

[a]*Department of Chemistry and Biochemistry, University of Notre Dame, 2365 Nieuwland Science Hall, Notre Dame, IN 46556, USA;* [b]*Beijing National Laboratory for Molecular Sciences, CAS Key Laboratory of Photochemistry, Institute of Chemistry, Chinese Academy of Sciences, Beijing 100190, P.R. China*

(*Received 7 January 2013; final version received 11 February 2013*)

A series of four related phenol derivatives, with 2,2′-dipicolylamine substituents at the ortho positions, were prepared and their $Zn^{2+}$ coordination complexes studied by spectroscopic methods. X-ray crystal diffraction analysis of a dinuclear zinc complex with two bridging acetate anions showed a ternary structure with highly charged interior and lipophilic exterior, which helps explain why this class of water-soluble complexes can effectively diffuse through cell membranes. The stability of the dinuclear zinc complexes in aqueous solution was found to be strongly anion dependent; that is, bridging oxyanions, such as acetate and pyrophosphate, lock the two $Zn^{2+}$ cations to the surrounding ligand and greatly enhance ligand/zinc affinity. Overall, the results provide new insight into the structural and mechanistic factors that control the recognition and chemosensing performance of phenoxide bridged dipicolylamine molecular probes.

**Keywords:** anion recognition; zinc coordination; nuclear magnetic resonance; X-ray crystallography; titration; spectroscopic analysis



## Introduction

Phenol derivatives with 2,2′-dipicolylamine (DPA) substituents at the ortho positions are known to readily form coordination complexes with $Zn^{2+}$, $Cu^{2+}$, $Ni^{2+}$, $Co^{3+}$, $Fe^{2+}$ and $Fe^{3+}$ cations, and quite a few X-ray crystal structures of dinuclear complexes have been described (*1*). This report focuses on the $Zn^{2+}$ complexes with generic molecular structure, **BDPA·Zn$_2$** (Scheme 1). These compounds are part of a larger family of $Zn^{2+}$–DPA complexes that have been developed for various supramolecular applications such as sensing of anionic biomolecules in aqueous solution, protein labelling, DNA targeting, RNA hydrolysis, biomembrane targeting and cell penetration (*2–4*). The long-term goal of our research is to invent new classes of molecular probes for biological imaging, and we have discovered that $Zn^{2+}$–DPA complexes have a remarkable ability to recognise anionic cell membrane surfaces selectively in complex biological environments such as cell culture and living animals (*5*). During these studies, we observed an unusual phase transfer feature with water-soluble **BDPA·Zn$_2$** complexes, namely, an ability to penetrate cell membranes (*6*). We exploited this finding by developing oligomers of **MDPA·Zn** as effective cell permeating peptides (*7*). However, non-selective cell penetration is not a desirable attribute for most bioimaging applications. In order to rationally improve the performance of **BDPA·Zn$_2$** complexes as bioimaging probes and chemical sensors, a better understanding of the fundamental coordination chemistry that controls the molecular recognition is needed.

Here, we report a study of the solid-state structure and solution dynamics of some **MDPA·Zn** and **BDPA·Zn$_2$** complexes using a combination of spectrometric methods. Specifically, we have examined the $Zn^{2+}$ complexation properties of four ligands, **L1**–**L4** (Scheme 1). We find that $Zn^{2+}$ affinity of these ligands in water is strongly anion dependent, that is, $Zn^{2+}$ affinity is greatly enhanced by the presence of bridging oxyanions, such as acetate ($OAc^-$) and pyrophosphate ($PPi^{4-}$). Furthermore, oxyanion bridging of the two $Zn^{2+}$ cations in **BDPA·Zn$_2$** produces a lipophilic ternary complex, which helps explain why water-soluble **BDPA·Zn$_2$** complexes can effectively diffuse through cell membranes. The article concludes with a discussion of how this study can be used to improve the performance of DPA coordination complexes as molecular imaging agents and optical chemosensors for $Zn^{2+}$ and oxyanions.

## Results and discussion

### *Synthesis and solid-state structures*

The ligands, **L1**–**L4**, were prepared in a straightforward fashion using established procedures that produced a Mannich reaction of the parent phenol with one or two molar equivalents of paraformaldehyde and DPA (*3c*). An X-ray crystal structure was obtained for the zinc acetate

*Corresponding author. Email: smith.115@nd.edu

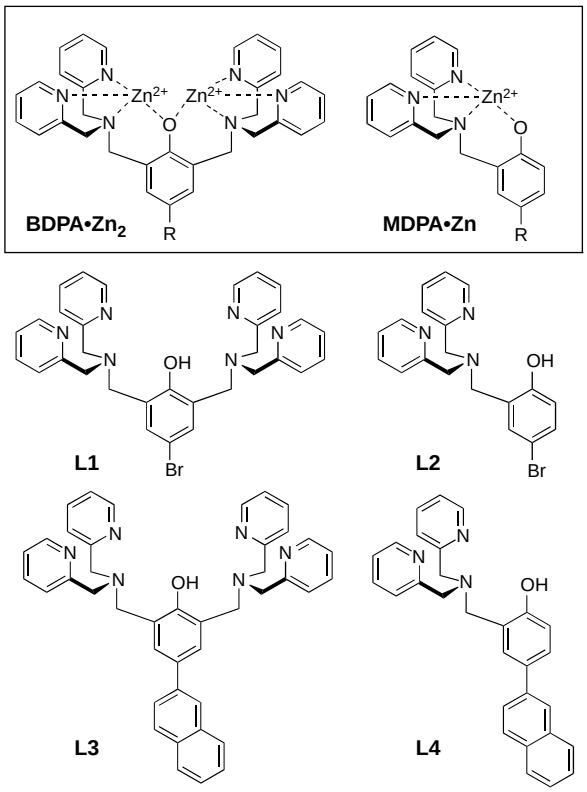


Scheme 1. Chemical structures.

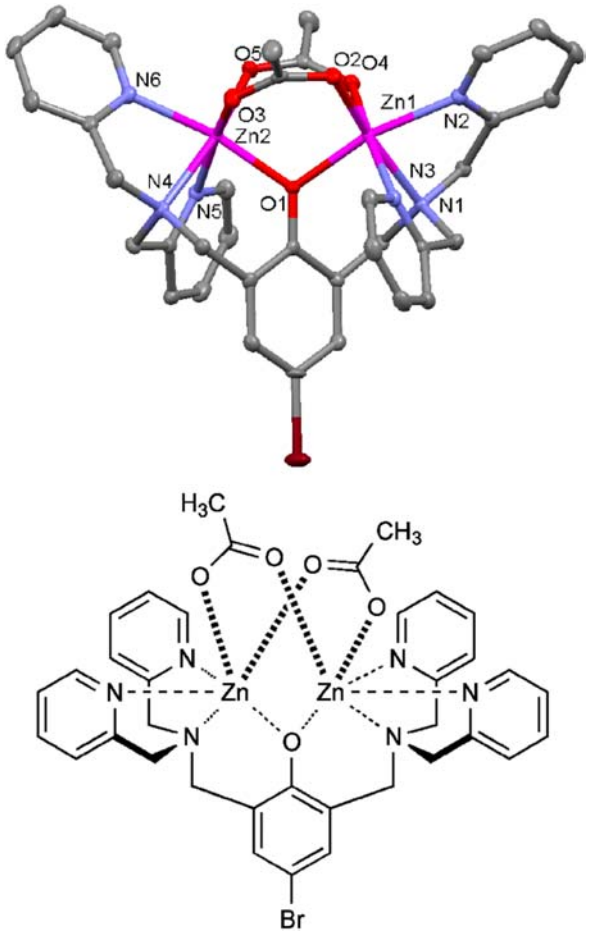


Figure 1. X-ray crystal structure of $Zn_2$**L1**$(OAc)_2(BF_4)$·2MeOH. The structure omits the $BF_4^-$ anion and two MeOH molecules for clarity. Thermal ellipsoids are indicated for all non-hydrogen atoms at the 50% probability level.

complex of **L1**. Single crystals were obtained by recrystallising a methanol solution containing **L1** mixed with two molar equivalents each of $Zn(OAc)_2$, triethylamine and $NaBF_4$ (*1a*). X-ray diffraction analysis revealed a molecular formula of $Zn_2$**L1**$(OAc)_2(BF_4)$·2MeOH. The $C_2$ symmetric structure (Figure 1) contains two, six-coordinate $Zn^{2+}$ centres with distorted octahedral geometries and an $N_3O_3$ donor set. Each $Zn^{2+}$ is coordinated by a DPA tertiary amine and two pyridyl nitrogen atoms, as well as the central phenoxy anion and two bridging $OAc^-$ anions. The average Zn–N distances are 2.23 Å for the Zn–tertiary amine interactions and 2.17 Å for the Zn–pyridyl nitrogen interactions. The average Zn—O distances are 2.04 Å for the Zn–phenoxy bonds and 2.05 Å for the Zn–acetoxy bonds. The *trans*-axial angles through the distorted octahedral Zn atoms are all in the range of 162–171°, and the Zn1···Zn2 distance is 3.36 Å. These bond lengths and angles are consistent with similar $Zn^{2+}$–DPA structures found in the literature (*1*). The molecular structure has a highly charged interior and lipophilic exterior, and suggests a structural process that enables partitioning of water-soluble **BDPA·Zn$_2$** complexes into vesicle and cell membranes (*7*). The process involves reversible association of **BDPA·Zn$_2$** complexes with one or two fatty acids or phospholipids at the membrane surface to produce membrane-soluble coordination complexes that are analogous to the structure in Figure 1.

### *Solution-state UV titrations*

The two phenolic ligands, **L3** and **L4**, have appended naphthalene chromophores and they are known to exhibit ratiometric spectral changes when they form zinc complexes (*3c*). Thus, **L3** and **L4** were chosen as sensing ligands for a study of the effects of bridging oxyanions on relative zinc complex stoichiometry and stability. Shown in Figure 2 are the results of an absorbance titration experiment in which $Zn(NO_3)_2$ was added to control mono-DPA ligand **L4** in methanol:water (4:1). There is a large bathochromic shift in absorption maxima as the ligand forms the expected **L4**:$Zn^{2+}$ salt structure (see **MDPA·Zn** in Scheme 1) with 1:1 stoichiometry. In the next set of absorbance titration experiments, $Zn(NO_3)_2$ was added to bis-DPA ligand **L3** in methanol:water (4:1)

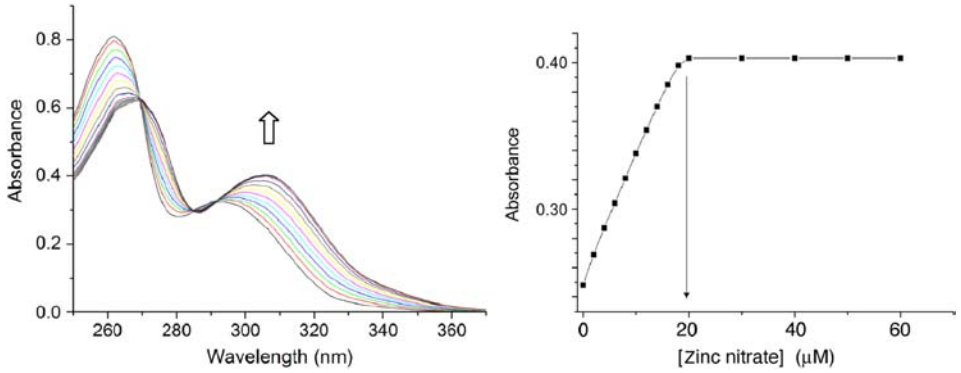


Figure 2. Left: absorbance spectra of **L4** (20 μM) upon titration of $Zn(NO_3)_2$ in methanol/water (4:1 volume ratio). Right: absorbance at 306 nm.

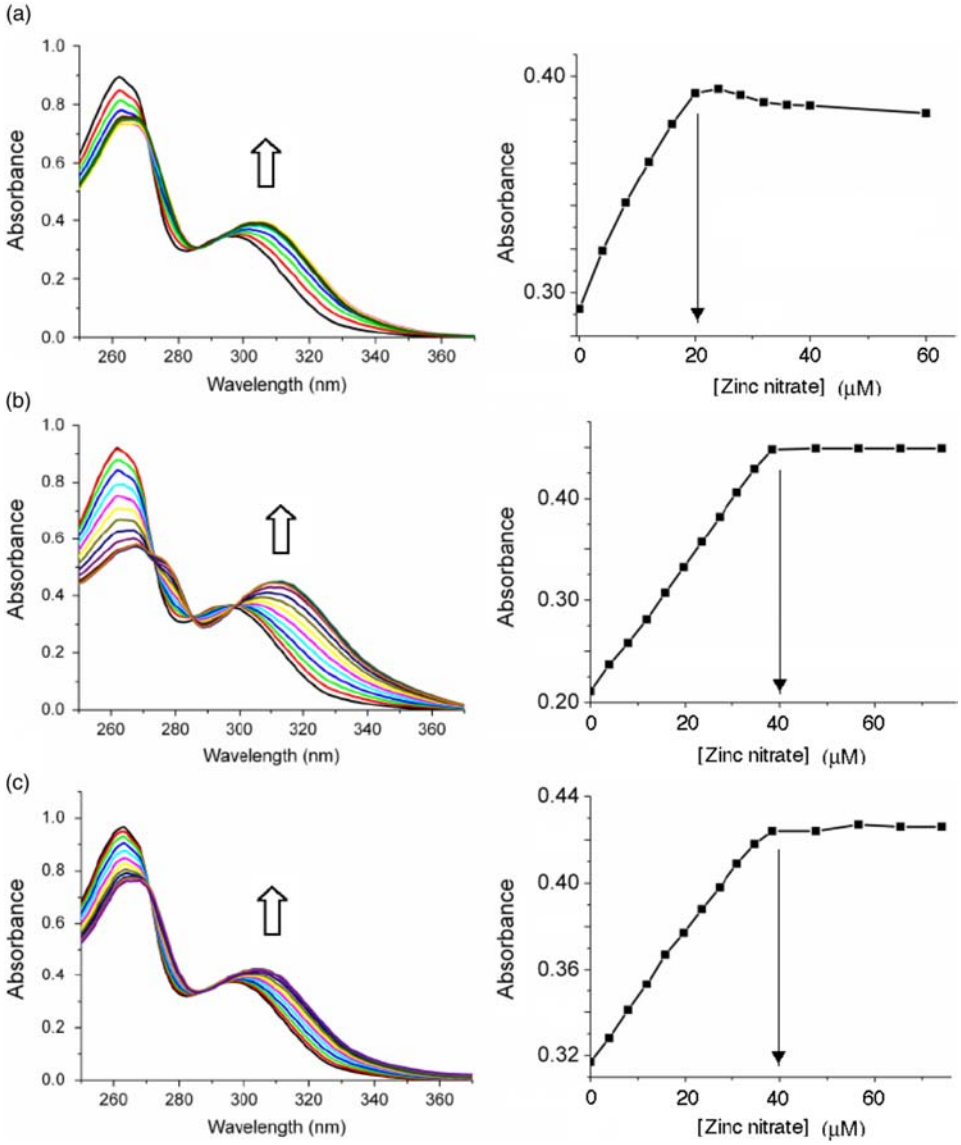


Figure 3. (a) Absorbance spectra of **L3** (20 μM) upon titration of $Zn(NO_3)_2$ in methanol/water (4:1 volume ratio); (b) same titration repeated in the presence of $Na_4PPi$ (40 μM) and (c) same titration repeated in the presence of NaOAc (40 μM). In each case, the graph on the right shows absorbance intensity change for the spectral wavelength maxima band.

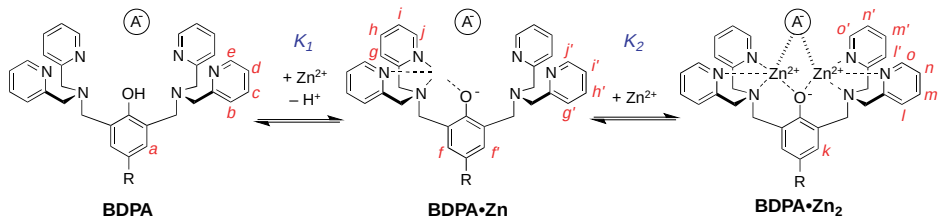


Scheme 2. Stepwise association of **BDPA** with $Zn^{2+}$ to form **BDPA·Zn₂** is pushed to the right by the presence of bridging oxyanions, $A^- = OAc^-$ or $PPi^{4-}$.

and yielded intriguing results. As shown in Figure 3, the stoichiometry at signal saturation depended on the identity of the counter anion. Addition of $Zn(NO_3)_2$ to a solution of **L3** reached saturation when the **L3**:$Zn^{2+}$ stoichiometry was 1:1 (Figure 3(a)). In contrast, the saturated **L3**:$Zn^{2+}$ stoichiometry was clearly in the ratio of 1:2 when the titration was conducted in the presence of $Na_4PPi$ (Figure 3(b)) or NaOAc (Figure 3(c)). The data are rationalised by considering the two stepwise, zinc association equilibria in Scheme 2. When the free **L3** ligand (represented as generic ligand **BDPA** in Scheme 2) is titrated with $Zn(NO_3)_2$, the first apparent $Zn^{2+}$ association constant, $K_1$, is larger than the second stepwise constant, $K_2$. Thus, the absorbance titration isotherm in Figure 3(a) reflects the first $Zn^{2+}$ association step in Scheme 2; that is, the conversion of free **BDPA** ligand into mononuclear zinc complex **BDPA·Zn**. When high-affinity, bridging oxyanions, such as $PPi^{4-}$ or $OAc^-$, are present in the solution, the second $Zn^{2+}$ association constant, $K_2$, is greatly enhanced such that it is larger than $K_1$ (Scheme 2). Thus, the absorbance changes in Figure 3(b),(c) reflect the conversion of generic ligand **BDPA** directly into dinuclear zinc complex **BDPA·Zn₂** with no measurable accumulation of the intermediate mononuclear zinc complex **BDPA·Zn**.

A meaningful quantitative analysis of the above absorption titration curves was not possible, primarily for two reasons – the aqueous methanol solvent was not buffered ($K_1$ is pH dependent) and the ligand/$Zn^{2+}$ association was too strong for the absorption titration method. However, semi-quantitative confirmation of the ligand/$Zn^{2+}$ stabilisation provided by the bridging oxyanions was gained by conducting competition experiments using ethylenediaminetetraacetic acid (EDTA) as a competitive $Zn^{2+}$ binder. The top of Figure 4 shows the change in absorption spectra when a solution of **L3**:2·$Zn(NO_3)_2$ in water/methanol (4:1) was titrated with two molar equivalents of EDTA. The spectra clearly show that the EDTA stripped the two zinc cations and produced the free **L3** ligand. In contrast, the set of spectra at the bottom of Figure 4 show that addition of two molar equivalents of $Na_4PPi$ to the solution of **L3**:2·$Zn(NO_3)_2$ greatly stabilised the dinuclear **L3**·$Zn_2$ structure and prevented EDTA stripping of the zinc cations. Even the addition of 100 molar equivalents of EDTA was unable to remove any measurable amount of $Zn^{2+}$. The data show clearly that $PPi^{4-}$, a strongly binding, bridging oxyanion, can stabilise the dinuclear **L3**·$Zn_2$ complex by several

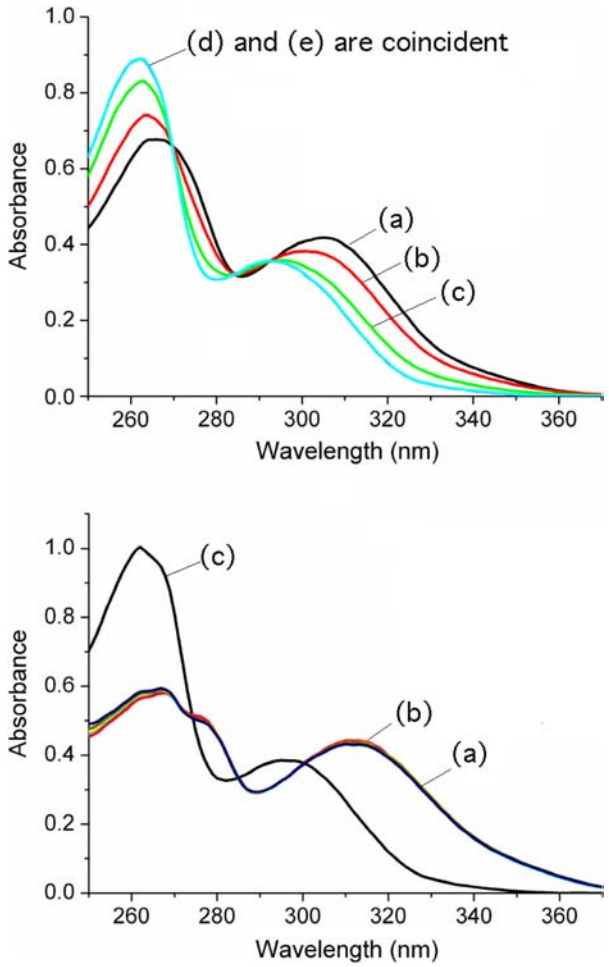


Figure 4. Top: absorption spectra of **L3**:2·$Zn(NO_3)_2$ complex (20 μM) showing complete conversion to **L3** upon addition of two molar equivalents of EDTA in water/methanol (4:1 volume ratio). (a) **L3**:2·$Zn(NO_3)_2$ with no EDTA, (b) **L3**:2·$Zn(NO_3)_2$ plus 0.5 equiv. EDTA, (c) **L3**:2·$Zn(NO_3)_2$ plus 1.0 equiv. EDTA, (d) **L3**:2·$Zn(NO_3)_2$ plus 2.0 equiv. EDTA, (e) **L3**. Bottom: absorption spectra of **L3**:2·$Zn(NO_3)_2$ complex (20 μM) in the presence of $Na_4PPi$ (40 μM) is unchanged by the addition of 100 molar equivalents of EDTA in water/methanol (4:1 volume ratio). (a) **L3**:2·$Zn(NO_3)_2$ plus $Na_4PPi$, (b) **L3**:2·$Zn(NO_3)_2$ plus $Na_4PPi$ and 100 equiv. EDTA and (c) **L3**.

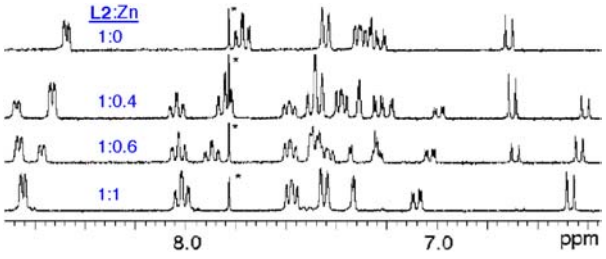


Figure 5. Partial $^1$H NMR spectra of **L2** (10 mM) with increasing amounts of $Zn(NO_3)_2$ in $CD_3OD/D_2O$ (4:1 volume ratio). The asterisk indicates a solvent peak.

orders of magnitude compared to a weakly binding anion such as $NO_3^-$.

### *Solution-state NMR titrations*

Additional structural evidence for the bridging anion stabilisation effect was obtained by monitoring analogous $Zn(NO_3)_2$ titration experiments using $^1$H NMR spectroscopy. Shown in Figure 5 are partial $^1$H NMR spectra from the titration of mono-DPA ligand **L2** with $Zn(NO_3)_2$ in $CD_3OD:D_2O$ (4:1). As expected, there was a smooth transition from free **L2** to **L2**:Zn complex with very strong affinity and 1:1 ligand/zinc stoichiometry. The two pyridyl rings in the DPA unit exhibit an equivalent set of four proton chemical shifts. Figures 6–8 show $^1$H NMR spectra obtained during the titration of bis-DPA ligand **L1** with $Zn(NO_3)_2$ in $CD_3OD:D_2O$ (4:1) under three different conditions, respectively: (i) no additional salt present, (ii) presence of NaOAc and (iii) presence of $Na_4PPi$. The peak assignments on the spectra refer to the atom labels in Scheme 2 as elucidated by analysing COSY spectra. The partial NMR spectra in Figure 6 show the titration of **L1** with $Zn(NO_3)_2$ with no other salt present. The first species to appear is the asymmetric **L1**:Zn complex with 1:1 stoichiometry. The most diagnostic peaks are the two aryl peaks on the central phenoxy ring which are non-equivalent at 6.98 and 7.25 ppm (assigned as *f* and *f′* on the generic mononuclear **BDPA·Zn** structure in Scheme 2). These peaks disappear as more $Zn(NO_3)_2$ is added, and they are replaced by the symmetric dinuclear **L1**:2·Zn complex. However, the pyridyl proton peaks are very broad, indicating a fluxional structure. The only sharp NMR peak is at 6.86 ppm and corresponds to the two equivalent protons on the central phenoxy ring (labelled as *k* on the generic **BDPA·Zn$_2$** structure in Scheme 2). The sodium salts of several anions were investigated to see if they influenced the zinc association equilibria. The presence of NaCl had no effect, with the titration spectra clearly showing stepwise production of the mononuclear species followed by the dinuclear complex (data not shown). In contrast, the presence of NaOAc promoted formation of the dinuclear zinc species with no evidence for any intermediate mononuclear structure. The spectra in Figure 7 show direct conversion of free **L1** into the dinuclear **L1**:2·Zn complex with eight, broadened inequivalent pyridyl proton signals. This spectral feature is consistent with the X-ray structure in Figure 1, which is a $C_2$ symmetric bis-acetoxy bridged complex with one zinc-coordinated pyridyl ring in pseudo-axial position and

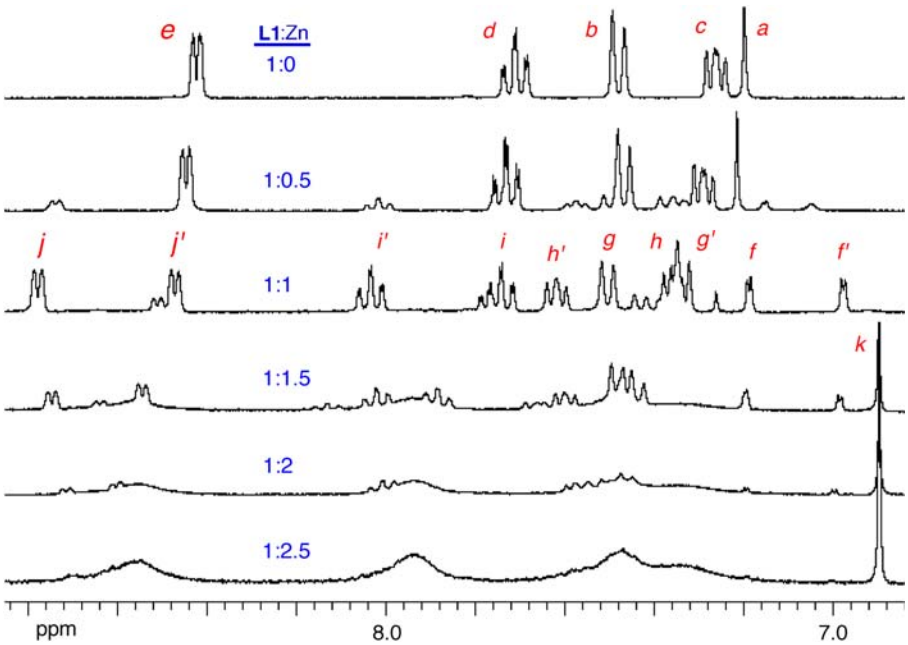


Figure 6. Partial $^1$H NMR spectra of **L1** (10 mM) with increasing amounts $Zn(NO_3)_2$ in $CD_3OD/D_2O$ (4:1 volume ratio).

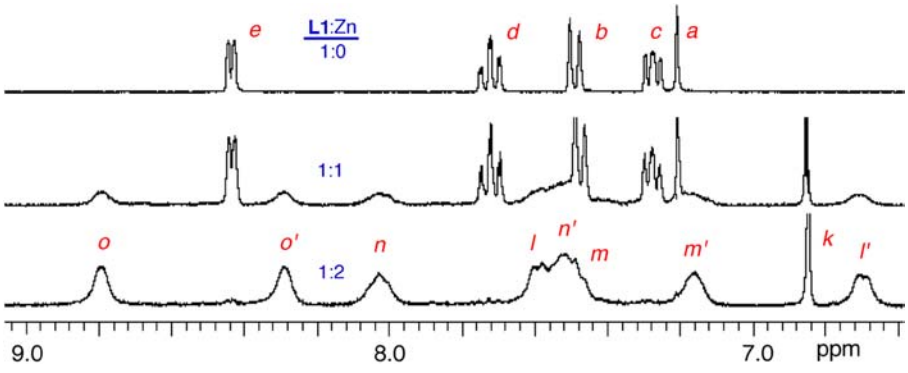


Figure 7. Partial $^1$H NMR spectra of **L1** (10 mM) in the presence of NaOAc (20 mM) with increasing amounts $Zn(NO_3)_2$ in $CD_3OD/D_2O$ (4:1 volume ratio).



the partner pyridyl ring in pseudo-equatorial position. The broadness of the pyridyl peaks indicates that the pyridyl rings undergo exchange of pseudo-axial/pseudo-equatorial $Zn^{2+}$-coordination positions. In Figure 8 is the titration of **L1** with $Zn(NO_3)_2$ in the presence of $Na_4PPi$. Again, the spectra show direct conversion of free **L1** into the dinuclear **L1**:2·Zn complex. In this case, the eight inequivalent pyridyl peaks of the dinuclear **L1**:2·Zn complex are quite sharp, indicating that the PPi strongly bridges the two zinc cations and produces a rigid, $C_2$ symmetric structure. Indeed, it is extremely likely that the structure is analogous to that shown in Figure 1 with a single tetradentate $PPi^{4-}$ replacing the two bidentate $OAc^-$ anions (*3b*,*d*). The increased rigidity of the $PPi^{4-}$ bridged structure is due to the higher anionic charge and stronger tetradentate zinc-coordination by the $PPi^{4-}$ which prevents the zinc–oxygen bond dissociation events that allow the pyridyl rings to exchange between pseudo-axial and pseudo-equatorial coordination positions.

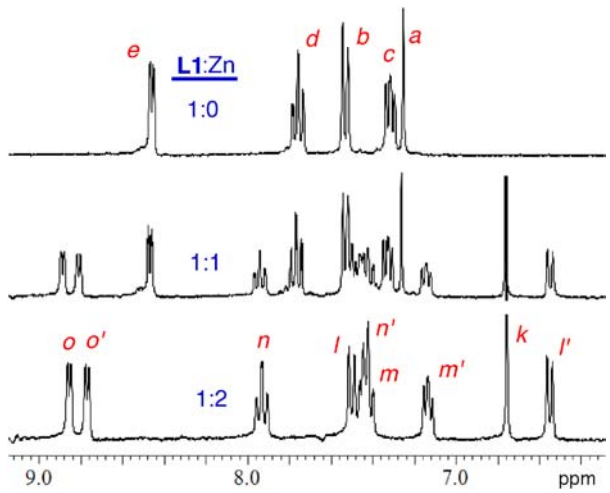


Figure 8. Partial $^1$H NMR spectra of **L1** (10 mM) in the presence of $Na_4PPi$ (20 mM) with increasing amounts $Zn(NO_3)_2$ in $CD_3OD/D_2O$ (4:1 volume ratio).

## Conclusions

The crystallographic and spectroscopic results demonstrate that strongly bridging oxyanions such as $OAc^-$ and $PPi^{4-}$ associate with water soluble, dinuclear **BDPA·Zn$_2$** complexes in aqueous solution and form relatively rigid, $C_2$ symmetric coordination structures with octahedral geometries around each $Zn^{2+}$ centre (Figure 1) (*1*, *3b*,*d*). It is reasonable to conclude that if the bridging anions were fatty acids or phospholipids, then the resulting coordination complexes would be lipophilic enough to partition into a biomembrane. The relatively high lipophilicity of DPA ligands has been reported by nuclear imaging researchers to produce poor pharmacokinetics and they have mitigated this problem by developing DPA analogues with increased hydrophilicity (*8*). It should be possible to refine these hydrophilic molecular designs and produce next-generation, membrane impermeable dinuclear zinc bis-DPA complexes with improved cell recognition and bioimaging performance.

The solution-state absorption and NMR titration data clearly show that bridging oxyanions lock the two $Zn^{2+}$ cations to the surrounding ligand and greatly enhance ligand/zinc affinity (Scheme 2). Thus, at sufficiently low zinc concentrations, the molecular recognition process can be viewed as a three-component assembly of mononuclear zinc–ligand complex, second $Zn^{2+}$ cation and bridging oxyanion. This stepwise process can be employed to create optical anion sensor designs that use the anion-mediated association of the second zinc cation to induce a change in ligand optical properties (*2c*, *5b*). At higher zinc concentrations, the bis-DPA ligand is saturated with both $Zn^{2+}$ cations (i.e. it exists entirely as a dinuclear **BDPA·Zn$_2$** complex), but the two sets of zinc-coordinated pyridyl rings are in a fluxional state. Association of a bridging oxyanion rigidifies the zinc-coordinated pyridyl rings, a process that may decrease non-radiative decay of excited state energy and be the basis of a 'turn on' fluorescent sensor design (*3c*, *9*). In addition to anion sensing, many DPA-containing receptors have been

investigated as $Zn^{2+}$ cation sensors and while it has been reported that the response of a bis-DPA $Zn^{2+}$ sensor can be anion dependent (*10*), the impact of this anion dependence on analytical performance for this class of zinc sensors has not been widely discussed. Finally, it is worth noting that the three-component molecular assembly described here mimics a common biological strategy for targeting the surface of biomembranes (*11*). Metal cations often act as bridging cofactors that enable membrane association of peripheral membrane proteins (e.g. membrane targeting by annexin V mediated by $Ca^{2+}$ ions) (*12*).

## Experimental

### *Synthesis*

The known ligands **L3** and **L4** were prepared by a literature method (*3c*), (an improved procedure is described in Ref. (*11*)), and ligands **L1** and **L2** were prepared by the following related procedure.

**L1**: A solution of 4-bromophenol (0.88 g), 1 M HCl (0.5 ml), paraformaldehyde (0.35 g) and DPA (2.1 g) in ethanol (20 ml) and water (40 ml) was refluxed for 36 h, then cooled to room temperature and neutralised with $Na_2CO_3$. The neutral suspension was extracted into chloroform, dried with sodium sulphate and the solvent was evaporated to yield a yellow oil that was purified on a silica gel column using an eluent of 97:3 $CHCl_3$:MeOH to give **L1** as a pale yellow oil (2.5 g), 83% yield. $^1$H NMR (300 MHz, $CDCl_3$, ppm): $\delta$ 8.53 (m, 4H), 7.61 (td, 4H, $J_1 = 7.8$ Hz, $J_2 = 1.8$ Hz), 7.44 (d, 4H, $J = 8.1$ Hz), 7.33 (s, 2H), 7.14 (m, 4H), 3.87 (s, 8H), 3.77 (s, 4H). $^{13}$C NMR (75 MHz, $CDCl_3$, ppm): $\delta$ 158.9, 155.1, 148.8, 136.6, 131.4, 126.5, 122.8, 122.0, 110.2, 59.7, 54.2. MS ($FAB^+$): HRMS $C_{32}H_{32}BrN_6O$ calcd. 595.1821, found 595.1832.

**L2**: The above procedure was used with the following stoichiometry: 4-bromophenol (0.88 g), 1 M HCl (0.5 ml), paraformaldehyde (0.35 g), DPA (1.0 g). The same work up and purification gave **L2** as pale yellow oil (1.7 g), 87% yield. $^1$H NMR (300 MHz, $CDCl_3$, ppm): $\delta$ 8.55 (m, 2H), 7.60 (td, 2H, $J_1 = 7.8$ Hz, $J_2 = 1.8$ Hz), 7.31 (d, 2H, $J = 7.8$ Hz), 7.22 (dd, 1H, $J_1 = 8.7$ Hz, $J_2 = 2.4$ Hz), 7.14 (m, 3H), 6.80 (d, 1H, $t = 8.7$ Hz), 3.87 (s, 4H), 3.74 (s, 2H). $^{13}$C NMR (75 MHz, $CDCl_3$, ppm): $\delta$ 157.8, 156.7, 148.6, 136.7, 132.4, 131.5, 125.0, 122.9, 122.1, 118.3, 110.1, 58.6, 56.1. MS ($FAB^+$): HRMS $C_{19}H_{19}BrN_3O$ calcd. 384.0711, found 384.0699.

### *X-ray crystallography*

***L1** dinuclear zinc acetate complex*. A solution of **L1** ligand and two molar equivalents of triethylamine, $Zn(OAc)_2$ and $NaBF_4$ in methanol was refluxed for 30 min and then allowed to cool to room temperature (*4a*). Colourless crystals were formed after 24 h and they were found to be suitable for X-ray diffraction analysis. $C_{38}H_{44}BBrF_4N_6O_7Zn_2$, $M_r = 994.25$, triclinic, unit cell dimensions $a = 10.2479(5)$, $b = 12.5046(6)$, $c = 17.2421(10)$ Å, $\alpha = 69.363(3)°$, $\beta = 81.066(3)°$, $\gamma = 86.542(3)°$, $V = 2042.60(18)$ Å$^3$, $T = 100(2)$ K, $P\bar{1}$, $Z = 2$. The structure was refined on $F_2$ to $wR_2 = 0.0809$, conventional $R_1 = 0.0310$ [11,493 reflections with $I > 2\sigma(I)$], and a goodness of fit = 1.055 for 10,254 refined parameters. The asymmetric unit contains the $Zn_2$**L1** complex coordinated by two OAc anions, one $BF_4$ anion, and two molecules of $CH_3OH$. One of the $CH_3OH$ molecules is disordered over two sites, and site occupancy for the principal component is 0.872(70).

### *Absorption titrations*

Appropriate aliquots of $Zn(NO_3)_2$ solution (20 mM in 4:1 $CH_3OH$:$H_2O$ volume ratio) were added to 3.0 ml solutions of ligand **L3** or **L4** in the presence or absence of NaCl, NaOAc or $Na_4PPi$ in the same solvent and the absorption spectrum acquired at 25°C.

### *$^1$H NMR titrations*

Appropriate aliquots of $Zn(NO_3)_2$ solution (100 mM in 4:1 $CH_3OD$:$D_2O$ volume ratio) were added to 0.75 ml solutions of ligand **L1** or **L2** in the presence or absence of NaCl, NaOAc or $Na_4PPi$ in the same solvent and the $^1$H NMR spectrum acquired at 25°C.

## Supporting Information Available

NMR assignments and CIF file for X-ray structure can be obtained via http://www.tandfonline.com. The crystallographic data is also provided in CCDC 901795, which can be obtained free of charge via http://www.ccdc.cam.ac.uk/conts/retrieving.html (or from the Cambridge Crystallographic Data Centre, 12 Union Road, Cambridge CB21EZ, UK; fax (+44) 1223-336-033; or deposit@ccdc.cam.uk).

## Acknowledgements

This work was supported by the University of Notre Dame and the NIH (USA). We are grateful to B. Noll and A. Oliver for acquiring and analysing the X-ray data.

## References

(1) (a) Adams, H.; Bradshaw, D.; Fenton, D.E. *Inorg. Chim. Acta* **2002**, *332*, 195–200; (b) Matsufuji, K.; Shiraishi, H.; Miyasato, Y.; Shiga, T.; Ohba, M.; Yokoyama T.; Okawa, H. *Bull. Chem. Soc. Jpn.* **2005**, *78*, 851–858; (c) Dalgaard, P.; Hazell, A.; McKenzie, C.J.; Moubaraki, B.; Murray, K.S. *Polyhedron* **2000**, *19*, 1909–1915; (d) Torelli, S.; Belle, C.;

Gautier-Luneau, I.; Pierre, J.L. *Inorg. Chem.* **2000**, *39*, 3526–3536; (e) Belle, C.; Beguin, C.; Gautier-Luneau, I.; Hamman, S.; Philouze, C.; Pierre, J.L.; Thomas, F.; Torelli, S. *Inorg. Chem.* **2002**, *41*, 479–491; (f) Suzuki, M.; Kanatomi, H.; Murase, I. *Chem. Lett.* **1981**, *10*, 1745–1748; (g) Seo, J.S.; Sung, N.-D.; Hynes, R.C.; Chin, J. *Inorg. Chem.* **1996**, *35*, 7472–7473; (h) Maeda, Y.; Ishida, A.; Ohba, M.; Sugihara, S.; Hayami, S. *Bull. Chem. Soc. Jpn.* **2002**, *75*, 2441–2448; (i) Albedyhl, S.; Averbuch-Pouchot, M.T.; Belle, C.; Krebs, B.; Pierre, J.-L.; Saint-Aman, E.; Torelli, S. *Eur. J. Inorg. Chem.* **2001**, 1457–1464; (j) Torelli, S.; Belle, C.; Gautier-Luneau, I.; Hamman, S.; Pierre, J.-L. *Inorg. Chim. Acta.* **2002**, *333*, 144–147; (k) Durot, S.; Hossain, L.H.; Hamman, S.; Jamet, H.; Orio, M.; Gautier-Luneau, I.; Luneau, D.; Philouze, C.; Pierre, J.-L.; Belle, C. *Inorg. Chem.* **2010**, *49*, 7832–7840.

(2) For reviews on molecular recognition using $Zn^{2+}$–DPA complexes, see: (a) Sakamoto, T.; Ojida A.; Hamachi, I. *Chem. Commun.* **2009**, *2*, 141–152, and references therein; (b) Kruppa, M.; König, B. *Chem. Rev.* **2006**, *106*, 3520–3560, and references therein; (c) O'Neil, E.J.; Smith, B.D. *Coord. Chem. Rev.* **2006**, *250*, 3068–3080, and references therein; (d) Kim, S.K.; Lee, D.H.; Hong, J.; Yoon, J. *Acc. Chem. Res.* **2009**, *42*, 23–31; (e) Zhou, Y.; Xu, Z.; Yoon, J. *Chem. Soc. Rev.* **2011**, *40*, 2222–2234; (f) Ngo, H.T.; Liu, X.; Jolliffe, K.A. *Chem. Soc. Rev.* **2012**, *41*, 4928–4965.

(3) For papers on molecular recognition using dinuclear **BDPA·Zn$_2$** complexes, see: (a) Han, M.S.; Kim, D.H. *Angew. Chem. Int. Ed.* **2002**, *41*, 3809–3811; (b) Lee, D.H.; Im, J.H.; Son, S.K.; Chung, Y.K; Hong, J.-I. *J. Am. Chem. Soc.* **2003**, *125*, 7752–7753; (c) Lee, D.H.; Kim, S.Y.; Son, S.K.; Chung, Y.K.; Hong, J.-I. *Angew. Chem. Int. Ed.* **2004**, *43*, 4777–4780; (d) Lee, J.H.; Park, J.; Lah, M.S.; Chin, J.; Hong, J.-I. *Org. Lett.* **2007**, *9*, 3729–3731; (e) Bae, S.W.; Cho, M.S.; Jeong, A.R.; Choi, B.R.; Kim, D.-E.; Yeo, W.-S.; Hong, J.-I. *Small* **2010**, *6*, 1499–1503; (f) Oh, D.J.; Kim, K.M.; Ahn, K.H. *Chem. Asian J.* **2011**, *6*, 2033–2038; (g) Liu, G.; Choi, K.Y.; Bhirde, A.; Swierczewska, M.; Yin, J.; Lee, S.W.; Park, J.H.; Hong, J.-I.; Xie, J.; Niu, G.; Kiesewetter, D.O.; Lee, S.; Chen, X. *Angew. Chem. Int. Ed.* **2012**, *51*, 445–449; (h) Honda, K.; Fujishima, S.-H.; Ojida, A.; Hamachi, I. *ChemBioChem* **2007**, *8*, 1370–1372; (i) Ojida, A.; Honda, K.; Shimi, D.; Kiyonaka, S.; Moria Y.; Hamachi, I. *J. Am. Chem. Soc.* **2006**, *128*, 10452–10459; (j) Honda, K.; Ojida A.; Hamachi, I. *Chem. Commun.* **2006**, 4024–4026. (k) Drewry, J.A.; Burger, S.; Mazouchi, A.; Duodu, E.; Ayers, P.; Gradinaru, C.C.; Gunning, P. T. *Med. Chem. Commun.* **2012**, *3*, 763–770.

(4) For papers on molecular recognition and catalysis using structurally related hydroxyl bridged dinuclear $Zn^{2+}$–DPA complexes, see: (a) Morrow, J.R.; Iranzo, O. *Curr. Opin. Chem. Biol*. **2004**, *8*, 192–200; (b) Ganesh, V.; Bodewits, K.; Bartholdson, S.J.; Natale, D.; Campopiano, D.J.; Marque-Rivas, J.C. *Angew. Chem. Int. Ed*. **2009**, *48*, 356–370; (c) Kinoshita, E.; Takahashi, M.; Takeda, H.; Shiro, M.; Koike, T. *Dalton Trans.* **2004**, *33*, 1189–1194; (d) Ciavatta, L.; Mareque, J.C.; Natale, D.; Salvatore, F. *Ann. Chim-Rome* **2006**, *96*, 317–325.

(5) (a) Koulov, A.V.; Stucker, K.; Lakshmi, C.; Robinson, J.P.; Smith, B.D. *Cell Death Differ.* **2003**, *10*, 1357–1359; (b) Koulov, A.V.; Hanshaw, R.G.; Stucker, K.A.; Lakshmi, C.; Smith, B.D. *Isr. J. Chem.* **2005**, *45*, 373–379; (c) Hanshaw, R.G.; Lakshmi, C.; Lambert, T.N.; Johnson, J.R.; Smith, B.D. *ChemBioChem.* **2005**, *6*, 2214–2220; (d) Leevy, W.M.; Gammon, S.T.; Johnson, J.R.; Lampkins, A.J.; Jiang, H.; Marquez, M.; Piwnica-Worms, D.; Smith, B.D. *Bioconjug. Chem.* **2008**, *19*, 686–692; (e) Smith, B.A.; Akers, W.J.; Leevy, W.M.; Lampkins, A.J.; Xiao, S.; Wolter, W.; Suckow, M.A.; Achilefu, S.; Smith, B.D.J. *Am. Chem. Soc.* **2010**, *132*, 67–69; (f) Smith, B.A.; Xiao, S.; Wolter, W.; Wheeler, J.; Suckow, M.A.; Smith, B.D. *Apoptosis* **2011**, *16*, 722–731; (g) Smith, B.A.; Xie, B.-W.; van Beek, E.R.; Que, I.; Blankevoort, V.; Xiao, S.; Cole, E.L.; Hoehn. M.; Kaijzel, E.L.; Löwik, C.W.G.M.; Smith, B.D. *ACS Chem. Neurosci.* **2012**, *3*, 530–537.

(6) (a) DiVittorio, K.M.; Leevy, W.M.; O'Neil, E.J.; Johnson, J.R.; Vakulenko, S.; Morris, J.D.; Rosek, K.D.; Serazin, N.; Hilkert, S.; Hurley, S.; Marquez, M.; Smith, B.D. *ChemBioChem*. **2008**, *9*, 286–293; (b) Jiang, H.; O'Neil, E.J.; DiVittorio, K.M.; Smith, B.D. *Org. Lett.* **2005**, *7*, 3013–3016.

(7) Johnson, J.R.; Jiang, H.; Smith, B.D. *Bioconjug. Chem.* **2008**, *19*, 1033–1039.

(8) Maresca, K.P.; Marquis, J.C.; Hillier, S.M.; Lu, G.; Femia, F.J.; Zimmerman, C.N.; Eckelman, W.C.; Joyal, J.L.; Babich, J.W. *Bioconjug. Chem.* **2010**, *21*, 1032–1042.

(9) For a discussion of other mechanisms that may control the fluorescence signal, see: Pathberiya, L.G.; Barlow, N.; Nguyen, T.; Graham, B.; Tuck, K.L. *Tetrahedron* **2012**, *68*, 9435–9439.

(10) Jang, Y.J.; Jun, E.J.; Lee, Y.J.; Kim, Y.S.; Kim, J.S.; Yoon, J. *J. Org. Chem.* **2005**, *70*, 9603–9606.

(11) Hanshaw, R.G.; Stahelin, R.V.; Smith, B.D. *Chem. Eur. J.* **2008**, *14*, 1690–1697.

(12) Lambert, T.N.; Smith, B.D. *Coord. Chem. Rev.* **2003**, *240*, 129–141.

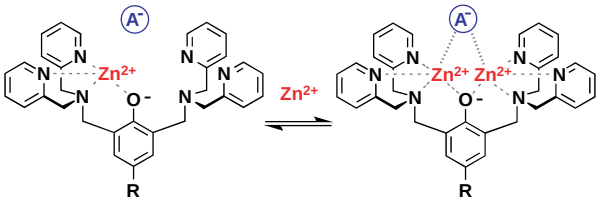


Dinuclear complex stability is strongly anion dependent; that is, bridging oxyanions lock the two zinc cations to the surrounding ligand and greatly enhance ligand/zinc affinity.

Edward J. O'Neil, Hua Jiang and Bradley D. Smith

Effect of bridging anions on the structure and stability of phenoxide bridged zinc dipicolylamine coordination complexes

**1–9**